



## Thrombolysis: Observations and numerical models

Remy Petkantchin <sup>a,\*</sup>, Raymond Padmos <sup>b</sup>, Karim Zouaoui Boudjeltia <sup>c</sup>, Franck Raynaud <sup>a</sup>, Bastien Chopard <sup>a</sup>, the INSIST investigators

<sup>a</sup> Scientific and Parallel Computing Group, Computer Science Department, University of Geneva, Switzerland

<sup>b</sup> Computational Science Laboratory, Institute for Informatics, Faculty of Science, University of Amsterdam, The Netherlands

<sup>c</sup> Laboratory of Experimental Medicine (ULB222), Faculty of Medicine, Université libre de Bruxelles, CHU de Charleroi, Belgium

### ARTICLE INFO

#### Keywords:

Ischemic Stroke  
Thrombolysis  
Numerical modeling

### ABSTRACT

This perspective paper considers thrombolysis in the context of ischemic strokes, intending to build eventually a numerical model capable of simulating the thrombolytic treatment and predicting patient outcomes. Numerical modeling is a scientific methodology based on an abstraction of a system but requires understanding their spatio-temporal interactions. However, although important, the current knowledge on thrombolysis is fragmented in contributions from which it is difficult to obtain a complete picture of the process, especially in a clinically relevant setup. This paper discusses, from a general point of view, how to develop a numerical model to describe the evolution of a patient clot under the action of a thrombolytic drug. We will present critical, yet fundamental, open questions that have emerged during this elaboration and discuss original experimental observations that challenge some of our current knowledge of thrombolysis.

### 1. Introduction

Ischemic stroke, first cause of disability and the third cause of death in civilized countries (INSIST consortium, 2017), happens when a brain artery gets blocked by an aggregate, a thrombus, of blood components, mostly fibrin, red blood cells (RBCs), and platelets, among others. Although thrombi result from the natural coagulation process, which is central to preventing bleeding, they have a dramatic effect when occluding brain arteries by impeding the transport of oxygen and nutrients to the brain. These obstructing thrombi can have different etiology: they can be formed either on the occlusion site (*atherothrombotic*) or somewhere else (*embolic*) and be dislodged from there to the brain. Treatment options are thrombolysis alone or combined with thrombectomy. The latter, in which safety and efficacy were demonstrated in 2015, consists in the mechanical removal of the blood clot through intravascular access (Berkhemer et al., 2015). The thrombolytic treatment, generally administrated within few hours after the onset of stroke symptoms, produces a chemical breakdown of the clot. This is typically obtained by injecting anti-coagulant, such as tissue-Plasminogen-Activator molecules (tPA), which binds to fibrin and facilitates the conversion of plasminogen to plasmin, a molecule that cleaves the fibrin strands. Although the biochemistry of thrombolytic treatment is well characterized, and plasmin-mediated fibrin lysis is shown to be efficient (Lansberg et al., 2009), its success rate remains unexplained very low with only 30% of the patients who

fully recover 3 months after treatment (Rull). The objective of the H2020 European INSIST project is to build from generated virtual populations *in silico* models for acute ischemic stroke, its treatment, and the resulting perfusion changes (Konduri et al., 2020). Under the umbrella of INSIST, the consortium aims to develop novel models of thrombolysis to identify the most critical factors responsible for the low positive outcome of chemical stroke treatment. In the past decades, intensive efforts have been made to address the question of thrombolysis from a modeling perspective (Anand et al., 2005; Bajd and Serša, 2013; Bannish et al., 2014; Miyazaki and Yamaguchi, 2003; Piebalgs and Xu, 2015; Piebalgs et al., 2018; Prasad et al., 2006; Gu et al., 2019). However, while constructing such a model in clinically relevant conditions, several questions were raised. The answers to some of them seem to be present in previous works, only sparsely or incompletely. Some others, including most fundamental ones, were found to be still open questions, hence revealing our lack of baseline knowledge as one attempt to simulate thrombolytic treatment in realistic physiological conditions.

The present opinion paper aims to gather information to answer these fundamental questions, highlighting these missing pieces of knowledge to encourage new experimental and clinical works. We propose to articulate our discussion around the elaboration of a numerical model of thrombolysis. This story arc has the advantage of covering most aspects of thrombolytic treatment, from patients specificity to the

\* Corresponding author.

E-mail address: [remy.petkantchin@unige.ch](mailto:remy.petkantchin@unige.ch) (R. Petkantchin).

more general biochemistry of lysis, and effectively highlighting what is known, hypothesized, or unknown about thrombolysis.

## 2. Model construction

For the non-specialized audience, we first present the general principles of constructing a numerical model using the context of simulating thrombolytic treatment. Elaborating on a model implies asking questions but also making choices to approach the problem which is considered. Among them, we note the need to adopt a particular point of view, placing oneself at one or more space and time scales, and to select a particular modeling framework (based for instance on differential equations, or multiagent systems, or cellular automata, etc.), which can be approached with different levels of formalism. It is possible to prioritize these different points of view, which in our opinion, depends on the availability of experimental data. First, without experiments, the role of the model is limited to imitate a natural process. Then, improving our knowledge allows one to reproduce the phenomenon in more details. Ultimately we expect the model to predict the outcome given the initial state of the system and, after calibration and validation, to formulate and explore novel hypotheses about the phenomenon of interest. Inherently, simulating thrombolysis in stroke events faces dramatic experimental issues and therefore is incredibly challenging. The initial conditions are almost unknown; probing real-time at the hospital, patients in an emergency state is unthinkable, and, in case of a positive outcome, the thrombus would have disappeared. If the chemical treatment is not successful, the patients undergo thrombectomy, severely damaging the retrieved clot.

Critical questions also emerge while choosing space and time scales at which we want to represent the system. Regarding modeling thrombolytic treatment, shall we consider time evolution associated with the binding of proteins, the heartbeats, lysis of the clot (about hundreds of minutes, [Bembenek et al., 2017](#); [Kim et al., 2015](#); [Diamond and Anand, 1993](#); [Diamond, 1999](#)), medical care of a patient? Similarly, the choice of space discretization is not trivial. The typical diameter of fibrin fibers is around  $10^{-8}$  to  $10^{-7}$  m, while typical thrombus length is centimetric. At the pore-scale, *i.e.* the space between fibers, one would have to divide the space of the simulation into  $\sim 10^{10}$  intervals, which is hardly feasible in terms of computational resources. To breach with the difficulties associated with the different scales involved, one possibility is to operate at an intermediate level, that is to say, at a mesoscopic scale. This means that microscopic details can be embedded in effective parameters of the model, whereas the macroscopic spatio-temporal evolution emerges from the computation, the macroscopic quantities being measured from averages of the mesoscopic ones. For our discussion, we rely on the lattice-Boltzmann method as a mesoscopic framework, a powerful and flexible numerical solver (see for instance [Krüger et al., 2017](#)), including biomedical problems ([Kotsalos et al., 2019](#); [Li et al., 2019](#); [Malaspinas et al., 2015](#)). Previous thrombolysis models ([Anand et al., 2005](#); [Bajd and Serša, 2013](#); [Bannish et al., 2014](#); [Miyazaki and Yamaguchi, 2003](#); [Piebalgs and Xu, 2015](#); [Piebalgs et al., 2018](#); [Prasad et al., 2006](#); [Gu et al., 2019](#)) considered these different scales, thus highlighting that there is still no consensus to prefer a microscopic over a macroscopic vision of the process (or *vice versa*). Interestingly, mesoscopic approaches seem to be absent from the literature. One may hypothesize that this scale requires knowing details from both the microscopic and the macroscopic worlds. Put it another way, while microscopic (resp. macroscopic) models can discard what happens at macroscopic (resp. microscopic) scales, the mesoscopic approach cannot compromise and needs to embrace a certain amount of those two.

The minimal set of components that we have to incorporate in our mesoscopic thrombolysis model is the following. First, we must account for the blood flow, especially how it is disrupted by the clot and restored after its dissolution. In the circulatory system, the blood is driven by pressure drop, and it appears that the physiological values of

this pressure drop are one of the open questions. The second component is the clot. Its composition has been recently detailed ([Staessens et al., 2020](#)), but the heterogeneity has not been yet addressed in computational models. Generally, it is described as a porous medium whose porosity depends on the composition. However, we will see that there is not much information about the porosity (and the permeability) of clots, whereas it directly affects the transport of lytic agents through the thrombus, and eventually, its degradation. Finally, the degradation of the clot itself has to be considered. In a mesoscopic approach, one does not need to detail all the reactions of the thrombolysis. Instead it is sufficient to adjust the reaction constants, corresponding to the aforementioned effective parameters, in order to mimic the different biochemical reactions in place (e.g., the binding of tPA and plasminogen, the conversion of bound plasminogen into plasmin, and the degradation of the clot by plasmin), as well as the time lag each of them induces. A schematic representation of the different components of the model can be seen in [Fig. 1](#), and a typical readout of a 3D mesoscopic simulation in [Fig. 2](#).

### 2.1. Blood flow conditions

The blood flow is driven through the body by the heart, which acts as a pump in the circulatory system. From a modeling perspective, it means that relevant physiological representation consists in imposing a pressure drop at the boundary of the system (the artery) rather than a velocity or flow rate. From simple biological and mechanical considerations, it is possible to guess the bounds for this pressure drop. A lower boundary could be estimated as the Poiseuille pressure gradient, generated by the resistance of the artery only, unobstructed. For a typical cerebral flow rate of 750 ml/min and considering a typical diameter of artery of 1 cm, the Poiseuille pressure gradient would be of the order of 200 Pa/m. An upper boundary would be reached if there is total blockage of the vessel. In that case, the pressure drop across the thrombus would be close to the systolic–diastolic blood pressure difference, and could not be higher than that. For a typical thrombus of length 1 cm and an average blood pressure, this gives a pressure gradient across the thrombus of the order of  $10^6$  Pa/m. The range between these two values is near four orders of magnitude, and the mean pressure gradient measurements across a thrombus in clinical conditions were barely present in the literature. This sparse knowledge is problematic when modeling realistic stroke situations. To date, very few clinical studies provide information about the pressure drop across a blocked artery. In [Sorimachi et al. \(2011\)](#), the authors found that these pressure drops were very close to the upper limit, which means high blockage of flow by the thrombus. However, numerical are at odds with each other. For instance, in [Piebalgs and Xu \(2015\)](#) the authors considered pressure differences between 1 and 20 Pa while in [Diamond and Anand \(1993\)](#) and [Shibeko et al. \(2020\)](#) used values up to 400 times larger (for a thrombus of 1 cm). Furthermore, these models assume a constant drop, while as lysis occurs, the pressure imposed at the inlet must be adapted because of the restoration of the flow. This flow restoration is usually called recanalization. Without any experimental measurements, assuming a constant drop is a fair assumption but is not entirely satisfying. One possibility to overcome this difficulty is to rely on a full brain circulatory model such as the one developed within the INSIST project by [Padmos et al. \(2021\)](#). As lysis progresses, the thrombus becomes more permeable. So by measuring the pressure drop across the thrombus, for a range of permeabilities, it is possible to estimate how the pressure drop will vary during recanalization. We illustrate this dependency in [Fig. 3](#) right. It is worth to notice that the pressure drop range measured for a generic Middle Cerebral Artery (MCA) - M1 segment occlusion (which accounts for most of the clinical cases) and clot length 5 mm, includes the clinical measurements of [Sorimachi et al. \(2011\)](#). This simulation approach offers a way to estimate the pressure drops across the thrombus, considering the collateral vessels and a progressive recanalization. However, this does

not compensate for the need for experimental data on pressure drop evolution during lysis. The only other numerical model which accounts for the pressure drop variation as the lysis proceeds is the one presented in [Piebalgs et al. \(2018\)](#).

The flow in the vessels surrounding the occluded one plays an important role ([Shibeko et al., 2020](#); [Santos et al., 2016b](#)) and is considered a good predictor for successful recanalization with profibrinolytic injection therapy ([Wufuer et al., 2017](#)). However, this is only a qualitative indicators, “good” or “bad”, estimated from medical imaging, and there is no quantitative description of the effect of collateral flow on recanalization in the treatment perspective. A recent work from INSIST partners ([Arrarte Terreros et al., under review](#)) identified up to 4 different patterns of flow in clotted regions of ischemic stroke patients: *slow anterograde*, *fast anterograde*, *retrograde* and mixed *anterograde-retrograde* flows. These different flow patterns surely affect the transport of lytic drugs to the occlusion site, and eventually the evolution of the lysis. Unfortunately, we are lacking quantitative clinical data, which complicates the validation of computational models and leaves the question of lysis outcome in complex geometries, an open (theoretical) problem yet critical from medical perspectives.

## 2.2. Thrombus description

One of the most important quantities to know when studying the lysis of thrombi is the resistance to flow establishment. High resistance to flow will lead to poor blood perfusion, hypoxia, and eventually necrosis of brain cells and limit lytic agents reaching the clot. Knowing how much the thrombus blocks the fluid would inform how much lytic agent could reach the clot and is a crucial predictor of lysis time. The resistance to flow may be identified as the specific Darcy permeability  $k$  of the thrombus, which predicts the flow through the clot given the pressure gradient. However, permeability is not an intrinsic characteristic of a material. It emerges from the coupling between the flow and the void fraction in a sample (or porosity). Knowing the value of the porosity and the spatial organization of void regions, one can estimate the permeability from the resolution at the scale of the pores. However, considering that the pore-scale is about few microns and the clot size is centimetric, it is only possible to achieve at a disproportionate computational cost. On the other hand, relying on a macroscopic approach would require knowledge, or postulating, a permeability/porosity relationship for fibrous media. Some examples are Davies’ equation ([Davies, 1952](#)), which is an empirical relationship based on airflow through fibrous media at low Reynolds; Jackson–James equation ([Jackson and James, 1986](#)) which is the weighted average of the solution to the Stokes equation for flow through 2D periodic square arrays of cylinders; or Clague’s equation ([Clague et al., 2000](#)), a numerical solution of permeability of randomly organized fibrous media. However, none of these are specific to blood clots.

At the mesoscopic scale, it is possible to account for the porosity of the thrombus in a relatively intuitive and straightforward manner, assuming that each clot voxel obstructs a tunable fraction of the flow. Such a method was presented in [Walsh et al. \(2009\)](#) for generic treatment of porous media, but we propose to extend it to the specific case of an obstructed artery. In brief, the fraction of obstruction, or solid fraction  $\gamma$ , is defined at the scale of a voxel and depends on the local concentration of fibrin, that changes in time with the progress of the lysis ([Diamond and Anand, 1993](#)), or other thrombi components (platelets, RBCs or others). With this approach, the relationship between permeability and porosity is not specified but will emerge as a function  $k(\gamma)$ . Although appealing, the mesoscopic approach, like others, hits the wall of our limited clinical knowledge regarding the permeability of a blood clot. The closest study (that we are aware of) to measuring blood clot permeability as a function of its solid fraction is the work of [Wufsus et al. \(2013\)](#). In their work, they measure the permeability of *in vitro* fibrin gels formed under static conditions (without any flow). Their results for pure fibrin gels, show good agreement

with Davies’ equation, but upon adding platelets, they found better agreement with Ethier’s model ([Ethier, 1991](#)). Overall, our knowledge remains limited regarding clot composition and permeability, with contradictory findings about whether the permeability of RBC-rich clots is higher or lower than platelet-rich clots ([Berndt et al., 2018](#); [Santos et al., 2016a](#); [Benson et al., 2020](#)). Furthermore, no studies show the effects of RBC deformation due to thrombus retraction ([Tutwiler et al., 2018](#)) or aging ([Zhou et al., 2014](#)) on thrombolysis. It is clear that computational models lack a well-defined model of thrombus permeability, and despite all experimental studies, it remains uncertain whether the permeability of *in vitro* fibrin clots and patient clots are comparable. To date, only one study from INSIST partners ([Arrarte Terreros et al., under review](#)) tries to measure *perviousness* from medical imaging data to quantify permeability. However, their results were 2 to 3 orders of magnitude lower than those of [Wufsus et al.](#), presumably due to artery compliance and the conditions of clot formation.

Not only the porosity of the thrombus but also its composition is necessary to simulate realistic blood clots. Histological analysis shows that clot composition varies substantially both in terms of composition and spatial localization ([Staessens and De Meyer, 2020](#); [Staessens et al., 2020](#)). Thus depending on patient history and thrombus origin and location ([Qazi et al., 2015](#)), thrombi can present RBC-rich/platelet-poor, mixed, or RBC-poor/platelet-rich features. The large composition spectrum observed in [Staessens and De Meyer \(2020\)](#) and [Staessens et al. \(2020\)](#) suggests that histological clot composition does not influence thrombolysis success, whereas it was shown that RBC-rich thrombi are easier to lyse ([Choi et al., 2018](#); [Kim et al., 2015](#)). Such controversial observations emphasize the need for more extensive investigation on the role of clot heterogeneity, including from modeling perspectives.

## 2.3. Lysis process

Most of the thrombolytic drugs are fibrinolytic drugs, and their role is to target specifically the fibrin strands that constitute the thrombus. The fibrinolytic role of plasmin ([Alkjaersig et al., 1959](#)) and the biochemistry underlying the conversion of plasminogen into its active form are known for decades ([Hoylaerts et al., 1982](#)). However, the modeling of the kinetics reactions remains a topical issue, and there is still no universal picture that has emerged to describe the process. Some of the models hypothesized quasistationary state between bound proteins to reduce the number of relevant equations ([Shibeko et al., 2020](#)), other discard bound species ([Kim et al., 2007](#)) or consider different level of binding sites accessibility on the fibers ([Diamond and Anand, 1993](#); [Piebalgs and Xu, 2015](#); [Raynaud et al., 2021](#)). Those models were somehow compared with experiments, but the lack of available experimental and clinical data is still an issue. For instance, in [Piebalgs and Xu \(2015\)](#), the authors relied on experimental data extracted from previous works published more than 30 years ago ([Rijken et al.](#)). When published experimental results can be found, they neither completely match the modeled system nor correspond with physiological data, making model validation and calibration a real tour de force. This issue is neither methodological nor technical but is inherent to the disease and treatment themselves. How can one have access to *in situ* physiological information when the thrombus is gone after a positive response to treatment? How to know the “true” initial conditions when mechanically retrieved clots have already been exposed to thrombolytic drugs?

From a modeling perspective, it is necessary to know the boundary conditions for the concentration of lytic agents. In clinical terms, it means knowing how much tPA will reach and react with the clot. However, this is hard to assess as it depends highly on the administration regime and patient-specific properties, such as density of collateral vessels or thrombus permeability. For example, in [Padmos et al. \(2021\)](#) the authors show in a 1D brain circulatory model that after about a minute, a fixed concentration at the inlet of the MCA is retrieved at the inlet of the occluded site ([Fig. 5](#)). These results were obtained using

**Table 1**

Physical values encountered in the literature for clotted artery-like systems. Plain values come directly from the corresponding source.

Paper	System	$\Delta P$ [Pa]	$L_{clot}$ [m]	$\nabla P$ [Pa/m]	$v_{seep}$ [m/s]	$k$ [m <sup>2</sup> ]
Diamond and Anand (1993)	<i>in vitro</i> fibrin gels	$7 \cdot 10^3$ <sup>b</sup>	$10^{-2}$ <sup>b</sup>	$7 \cdot 10^5$	$10^{-5}$ to $10^{-1}$ <sup>a</sup>	$10^{-16}$ to $10^{-12}$
Wufusus et al. (2013)	<i>in vitro</i> fibrin gels	$10^2$ to $10^4$ <sup>b</sup>	$10^{-2}$ <sup>b</sup>	$10^4$ to $10^6$	$10^{-6}$ to $10^{-4}$ <sup>a</sup>	$10^{-16}$ to $10^{-13}$
Sorimachi et al. (2011)	<i>in vivo</i> patients	$8 \cdot 10^3$	$10^{-2}$ <sup>b</sup>	$8 \cdot 10^5$ <sup>b</sup>		
Dutra et al. (2019)	<i>in vivo</i> patients		$10^{-2}$			
Arrarte Terreros et al. (under review)	<i>in vivo</i> patients		$10^{-2}$		$10^{-3}$ to $10^{-2}$	
Piebalgs and Xu (2015)	<i>in silico</i> based on Wu observation (Wu et al., 1994)	1 to 20	$2.5 \cdot 10^{-3}$	$10^3$	$10^{-3}$ <sup>a</sup>	$10^{-11}$

<sup>a</sup>Computed based on given parameters.<sup>b</sup>Computed based on given parameters, and assuming thrombi of length 1 cm.

Blank cells mean that the values are not given in the corresponding paper. Most studies agree on the typical clot length. Diamond's and Wufusus' pressure gradients applied *in vitro* seem to match Sorimachi's measure of *in vivo* pressure drop (before–after the thrombus). Terreros et al. however measure velocities 2 to 3 orders of magnitude different from Wufusus'. Finally, Piebalgs seem to use non-physiological values for the pressure drop, compared to Sorimachi.

an infusion administration, but patterns of administration can be more elaborated. The standard protocol (Reed et al., 2020) consists of 10% of the total dose as a bolus, followed by the remaining 90% as infusion over an hour. However, no study demonstrates its efficacy over others or whether the administration should be adapted to patient-specific cases. A full-blown model that aims to incorporate blood flow, realistic geometry artery, thrombus properties, would also need to integrate information about different patterns of drug administration. The latter can be estimated from a full circulatory model but will need further clinical evidence to deliver efficient and accurate thrombolysis models.

### 3. Conclusion

Despite a very advanced and detailed knowledge, in a context where the public health stakes are colossal, it is surprising to note that our global understanding of thrombolysis processes remains largely incomplete. This observation is all the more surprising given that specific aspects of the phenomena are known in great detail. However, when considering thrombolysis as a whole in a clinically relevant context, our knowledge is quickly limited, and open questions multiply.

This limitation can be attributed to the inherent difficulty of obtaining reliable experimental data with a generalizable scope, i.e., extracting information specific to a single patient. What we wish to highlight in this perspective article is the difficulty of first putting together the various elements, both from a clinical and theoretical point of view and second to put up a unified vision of the fundamental properties of thrombolysis, which results in hindering the possibility of developing credible models that can be calibrated, tested and validated.

Many computational approaches have already tackled the problem but have had to face the lack of experimental and *in vivo* data. Table 1 shows that there is barely a consensus for the most basic physical quantities. For example, the pressure gradient (driving the blood flow) and the permeability of clots (the primary source of resistance to blood flow) vary by several orders of magnitude depending on the study one considers. As problematic as the lack of experimental evidence, the contradictions between experimental observations make it very difficult to develop reliable models. For example, platelets appeared to be antifibrinolytic (Booth et al., 1988; Mosnier et al., 2003) or profibrinolytic (Baeten et al., 2010; Whyte et al., 2015) or both depending on the conditions of the patients (Fig. 4).

While the future of medical research is increasingly moving towards *in silico* approaches, from the generation of patient cohorts to the design of new drugs and treatments, we feel it is essential to recall that a numerical model, although an abstraction of a natural process, cannot be freed from a thorough and reliable knowledge of the elementary properties of the considered phenomenon. Moreover, the development of a new numerical model helps scientists to identify open questions and missing links between existing pieces of knowledge.

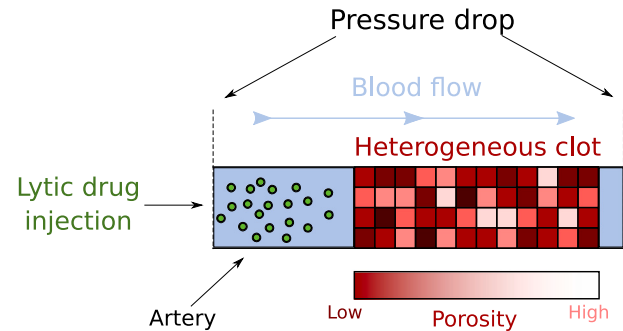


**Fig. 1.** General setup of a simulation. A cylindrical pipe represents the vessel in which the clot is placed. This pipe can be substituted with a patient-imported 3D vessel. The clot can have any shape, and its density is specified at voxel (volume element) scale ( $\sim 100 \mu\text{m}$  in this case). The colormap shows the porosity value for each clot voxel, which simulates heterogeneity. At the left and right boundaries, pressure is imposed, so a flow is driven by this pressure drop. Lytic agent, represented as packets of particles, is injected upstream of the clot. As these particles interact, the lysis occurs, and the clot will become more and more porous and permeable, until it breaks down completely.

### Declaration of competing interest

The authors declare that they have no known competing financial interests or personal relationships that could have appeared to influence the work reported in this paper.

### Acknowledgments

This research is part of the INSIST project (INSIST consortium, 2017), which has received funding from the European Union's Horizon 2020 research and innovation programme under grant agreement No. 777072.

### Appendix A. Material and methods for experiment presented in Fig. 4

Blood samples were collected from healthy volunteers (healthy subject:  $n = 28$ ), diabetic patients ( $n = 23$ ) and patients with previous venous thrombosis ( $n = 10$ ). The procedure was approved by the hospital ethics committee of the Centre hospitalier universitaire (CHU) de Charleroi, Belgium (Comité d'Ethique I.S.P.P.C: OM008). The studies conform to the principles outlined in the Declaration of Helsinki. Venous blood was drawn into tubes with 3.2% sodium citrate solution, at pH 7.4. Platelet-rich plasma (PRP) was obtained by a centrifugation of whole blood at 150 g for 10 min. For each donor, the platelet (plt) count of the PRP was adjusted at  $300.103 \text{ plt}/\mu\text{l}$  by dilution with the platelet-poor plasma (PPP) from this donor. PPP and PRP for each donor were put in a device dedicated to the fibrinolysis analysis

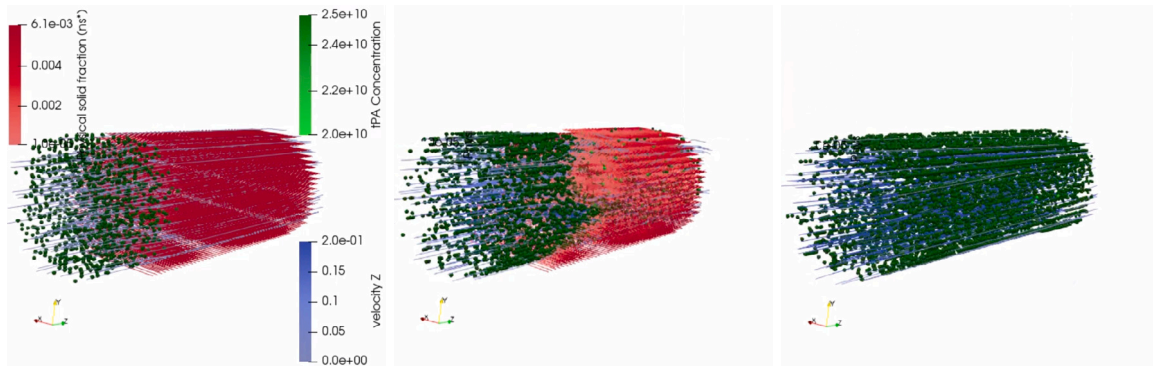


Fig. 2. Snapshots of a 3D mesoscopic thrombolysis model: A thrombus (in red) is blocking a cylindrical artery, profibrinolytic particles (in green) are transported by the blood flow (computed via the lattice-Boltzmann method, in blue). Left) Initial condition. Middle) Intermediate stage, the thrombus is degraded upon contact with profibrinolytic particles. Right) Lysis is finished and blood flow is restored. (For interpretation of the references to color in this figure legend, the reader is referred to the web version of this article.)

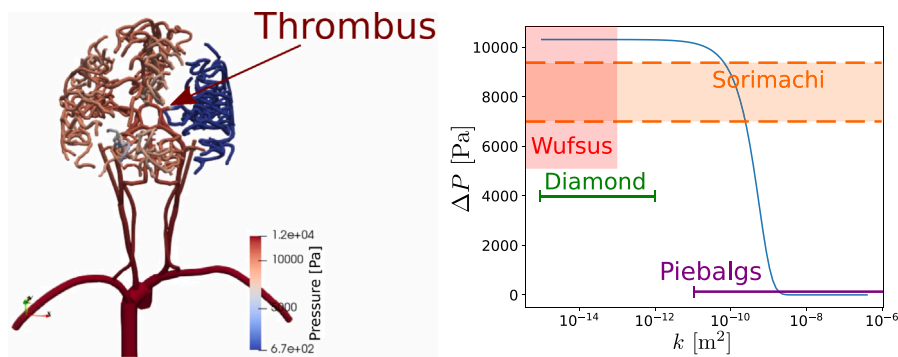


Fig. 3. 1D brain circulation simulation, based on Padmos et al.’s model (Padmos et al., 2021). (Left) A 5 mm long clot is placed in the left M1 segment, and generates a pressure drop. (Right) Dependency of the blood pressure difference  $\Delta P$  on the permeability  $k$  of the clot, for a 5 mm long occlusion, in a typical M1 segment of a MCA. Comparison with pressure drops measured by Sorimachi (orange area) (Sorimachi et al., 2005) (*in vivo*), Wufusus (red area) (Wufusus et al., 2013) (*in vitro*), and with ones used in the models of Diamond (green line) (Diamond and Anand, 1993) and Piebalgs (purple line) (Piebalgs and Xu, 2015). (For interpretation of the references to color in this figure legend, the reader is referred to the web version of this article.)

## Appendix B. Thrombolysis model

### B.1. Fluid solver

The open-source lattice-Boltzmann (LB) solver Palabos (Parallel Lattice Boltzmann Solver) (Latt et al., 2020) is used to simulate the blood flow transporting the lytic drug.

In our model, the domain is described with a regular D3Q19 lattice (3 spatial dimensions, 19 discrete velocities). For the sake of simplicity, the obstructed blood vessel is represented by a pipe of cylindrical shape, with rigid walls, but if needed, any patient-specific geometry can be imported.

Pressure boundary conditions were imposed on both ends of the artery, by imposing densities. As lysis occurs, the pressure imposed in inlet must be adapted, because recanalization occurs. It is adapted following the results presented in Fig. 3.

### B.2. Thrombus description

The thrombi in our model is described at a coarse scale, as voxels that obstruct more or less the flow, to mimic the observed resistance to flow. For now, these are only homogeneous fibrin thrombi. The fraction of obstruction, called solid fraction  $\gamma$  of the voxel, as defined by

Walsh (Walsh et al., 2009), is related to the LB populations as follows:

$$f_i^{out}(x, t) = (1 - \gamma)f_i^c(x, t) + \gamma f_i^{in}(x, t) \quad (1)$$

with  $f_i^{out}(x, t)$  the outgoing populations after the partially solid collision – or partially bounce-back (PBB) – computation, in lattice direction  $i$ , at position  $x$  and time  $t$ ,  $f_i^c(x, t)$  the populations immediately after the fluid collision step, and  $f_i^{in}(x, t)$  the incoming fluid packet before the collision step, in direction  $-i$ .  $\gamma$  can vary continuously from 0 (completely fluid voxel) to 1 (completely solid voxel).

Walsh et al. show that  $\gamma$  is related to the permeability  $k$  of the PBB voxel as follows:

$$k = \frac{(1 - \gamma)v dt}{2\gamma} \quad (2)$$

where  $v$  is the viscosity of the fluid and  $dt$  the time interval of the LB simulation.  $k$  and  $v$  are here in physical units.

As suggested in Walsh’s paper (Walsh et al., 2009), it is necessary to apply a mapping of a physical solid fraction  $n_s^*$  to the model solid fraction  $\gamma(n_s^*)$ , in order to obtain the desired permeability law. To do so, we simply invert relation (2):

$$\gamma = \frac{1}{1 + \frac{2k}{v dt}} \quad (3)$$

And we substitute the value of  $k$  with any function  $k(n_s^*)$  which describes the permeability law of the physical system of interest. This will, in turn, yield the desired  $\gamma(n_s^*)$  relationship. Data from Wufusus

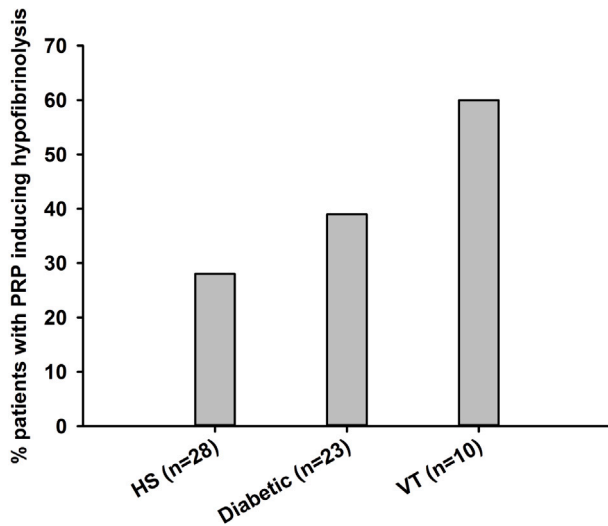


Fig. 4. Effect of platelets on plasma fibrinolysis. Fibrinolytic tests were performed on plasma poor (PPP) and rich in platelets (PRP; platelets adjusted to 300.103/ $\mu$ l). Results show the percentage of people presenting a hypofibrinolysis when their platelets were added in plasma. Three populations were studied: HS (healthy subjects), Diabetic patients (Diabetic) and patients with antecedent of venous thrombosis (VT).

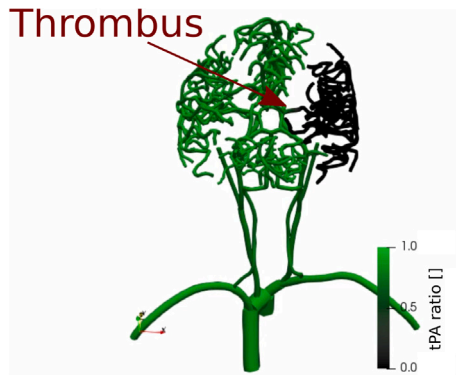


Fig. 5. Simulation of transport of tPA in the brain vasculature system, using Padmos et al. model (Padmos et al., 2021). The colormap shows the ratio of local tPA concentration, against tPA at perfusion site. After some time, the concentration of tPA is the same everywhere before the thrombus. (For interpretation of the references to color in this figure legend, the reader is referred to the web version of this article.)

et al. (2013) was used to make the choice of using Davies' law for the thrombus permeability model:

$$k_{\text{Davies}}(n_s^*) = R_f^2 (16n_s^{*1.5}(1 + 56n_s^{*3}))^{-1} \quad (4)$$

with fibrin fiber radius  $R_f$  ranging from 50 to 250 nm.

Finally,  $n_s^*$  is directly related to the fibrin density, by using Diamond et al.'s relationship (Diamond and Anand, 1993):

$$n_s^*(x, t) = \pi R_f^2(x, t) \frac{L_{\Delta V}}{\Delta V}, \quad (5)$$

where  $R_f(x, t)$  is the average fibrin fiber radius at position  $x$  and time  $t$ , and  $L_{\Delta V}$  is the total length of fibrin strands in volume  $\Delta V$ .

### B.3. Lysis model

Shibeko et al. (2020) modelize the thrombolysis process in a reduced model with 2 PDEs, 3 ODEs and 1 constraint equation. Their 6-equation model of thrombolysis was used, and further reduced to 2 equations. The only entities remaining in the present model, are fibrin

$F_n$  and a substitute for lytic agent, that we called anti-fibrin  $\tilde{F}n$ .

$$\frac{dF_n(x, t)}{dt} = -k_1 F_n(x, t) \cdot \tilde{F}n(x, t) \quad (6)$$

$$\frac{d\tilde{F}n(x, t)}{dt} = -k_2 F_n(x, t) \cdot \tilde{F}n(x, t) \quad (7)$$

where  $k_1$ ,  $k_2$  are the rates of degradation of fibrin and anti-fibrin respectively, upon interaction. These constants are meant to capture the effects of action of all other components normally present, as well as their delay of action.

### Appendix C. INSIST investigators

Charles Majoie<sup>1</sup>, Ed van Bavel<sup>2</sup>, Henk Marquering<sup>1,2</sup>, Nerea Arrarte-Terrerros<sup>1,2</sup>, Praneta Konduri<sup>1,2</sup>, Sissy Georgakopoulou<sup>2</sup>, Yvo Roos<sup>3</sup>, Alfons Hoekstra<sup>4</sup>, Raymond Padmos<sup>4</sup>, Victor Azizi<sup>4</sup>, Claire Miller<sup>4</sup>, Max van der Kolk<sup>4</sup>, Aad van der Lugt<sup>5</sup>, Diederik W.J. Dippel<sup>6</sup>, Hester L. Lingsma<sup>7</sup>, Nikki Boodt<sup>5,6,7</sup>, Noor Samuels<sup>5,6,7</sup>, Stephen Payne<sup>8</sup>, Tamas Jozsa<sup>8</sup>, Wahbi K. El-Bouri<sup>8</sup>, Michael Gilvarry<sup>9</sup>, Ray McCarthy<sup>9</sup>, Sharon Duffy<sup>9</sup>, Anushree Dwivedi<sup>9</sup>, Behrooz Fereidoonzehad<sup>10</sup>, Kevin Moerman<sup>10</sup>, Patrick Mc Garry<sup>10</sup>, Senna Staessens<sup>11</sup>, Simon de Meyer<sup>11</sup>, Sarah Vandelanotte<sup>11</sup>, Francesco Migliavacca<sup>12</sup>, Gabriele Dubini<sup>12</sup>, Giulia Luraghi<sup>12</sup>, Jose Felix Rodriguez Matas<sup>12</sup>, Sara Bridio<sup>12</sup>, Bastien Chopard<sup>13</sup>, Franck Raynaud<sup>13</sup>, Remy Petkantchin<sup>13</sup>, Vanessa Blanc-Guillemaud<sup>14</sup>, Mikhail Pantelev<sup>15,16</sup>, Alexey Shibeko<sup>15</sup>, Karim Zouaoui Boudjeltia<sup>17</sup>.

<sup>1</sup>Department of Radiology and Nuclear Medicine, Amsterdam UMC, location AMC, Amsterdam, the Netherlands; <sup>2</sup>Biomedical Engineering and Physics, Amsterdam UMC, location AMC, Amsterdam, the Netherlands; <sup>3</sup>Department of Neurology, Amsterdam UMC, location AMC, Amsterdam, the Netherlands; <sup>4</sup>Computational Science Lab, Faculty of Science, Institute for Informatics, University of Amsterdam, Amsterdam, the Netherlands; <sup>5</sup>Department of Radiology and Nuclear Medicine, Erasmus MC University Medical Center, PO Box 2040, 3000 CA Rotterdam, the Netherlands; <sup>6</sup>Department of Neurology, Erasmus MC University Medical Center, PO Box 2040, 3000 CA Rotterdam, the Netherlands; <sup>7</sup>Department of Public Health, Erasmus MC University Medical Center, PO Box 2040, 3000 CA Rotterdam, the Netherlands; <sup>8</sup>Institute of Biomedical Engineering, Department of Engineering Science, University of Oxford, Parks Road, Oxford OX1 3PJ, UK; <sup>9</sup>Cerenovus, Galway Neuro Technology Center, Galway, Ireland; <sup>10</sup>College of Engineering and Informatics, National University of Ireland Galway, Ireland; National Center for Biomedical Engineering Science, National University of Ireland Galway, Ireland; <sup>11</sup>Laboratory for Thrombosis Research, KU Leuven Campus Kulak Kortrijk, Kortrijk, Belgium; <sup>12</sup>Laboratory of Biological Structure Mechanics, Department of Chemistry, Materials and Chemical Engineering "Giulio Natta", Politecnico di Milano, Piazza Leonardo da Vinci 32, 20133 Milano, Italy; <sup>13</sup>Computer Science Department, University of Geneva, CUI, 7 route de Drize, 1227 Carouge, Switzerland; <sup>14</sup>Institut de Recherches Internationales Servier, Coubevoise Cedex, France; <sup>15</sup>Center for Theoretical Problems of Physicochemical Pharmacology RAS, Moscow, Russia; <sup>16</sup>Dmitry Rogachev National Research Center of Pediatric Hematology, Oncology and Immunology, Moscow, Russia; Faculty of Physics, Lomonosov Moscow State University, Moscow, Russia; <sup>17</sup>Laboratory of Experimental Medicine (ULB 222 Unit), Université Libre de Bruxelles (ULB), CHU de Charleroi, Belgium.

### References

- Alkjaersig, N., Fletcher, A.P., Sherry, S., 1959. The mechanism of clot dissolution by plasmin. *J. Clin. Invest.* 38 (7), 1086–1095.
- Anand, M., Rajagopal, K., Rajagopal, K.R., 2005. A model for the formation and lysis of blood clots. *Pathophysiol. Haemost. Thromb.* 34 (2–3), 109–120.
- Arrarte-Terrerros, N., Tolhuisen, M.L., Bennink, E., de Jong, H.W.A.M., Beenen, L.F.M., Majoie, C.B.L.M., van Bavel, E., Marquering, H.A., 2020. From perviousness to permeability, modelling and measuring intra-thrombus flow in acute ischemic stroke. *J. Biomech.* 111, 110001.

- Baeten, K.M., Richard, M.C., Kanse, S.M., Mutch, N.J., Degen, J.L., Booth, N.A., 2010. Activation of single-chain urokinase-type plasminogen activator by platelet-associated plasminogen: A mechanism for stimulation of fibrinolysis by platelets. *J. Thromb. Haemost.* 8 (6), 1313–1322.
- Bajd, F., Serša, I., 2013. Mathematical modeling of blood clot fragmentation during flow-mediated thrombolysis. *Biophys. J.* 104 (5), 1181–1190.
- Bannish, B.E., Keener, J.P., Fogelson, A.L., 2014. Modelling fibrinolysis: A 3D stochastic multiscale model. *Math. Med. Biol.* 31 (1), 17–44.
- Bembenek, J.P., Niewada, M., Siudut, J., Plens, K., Członkowska, A., Undas, A., 2017. Fibrin clot characteristics in acute ischaemic stroke patients treated with thrombolysis: The impact on clinical outcome. *Thromb. Haemost.* 117 (07), 1440–1447.
- Benson, J.C., Fitzgerald, S.T., Kadirvel, R., Johnson, C., Dai, D., Karen, D., Kallmes, D.F., Brinjikji, W., 2020. Clot permeability and histopathology: Is a clot's perviousness on CT imaging correlated with its histologic composition? *J. Neuro Interv. Surg.* 12 (1), 38–42.
- Berkhemer, O.A., Fransen, P.S.S., Beumer, D., van den Berg, L.A., Lingsma, H.F., Yoo, A.J., Schonewille, W.J., Vos, J.A., Nederkoorn, P.J., Wermer, M.J.H., van Walderveen, M.A.A., Staals, J., Hofmeijer, J., van Oostayen, J.A., Lycklama à Nijeholt, G.J., Boiten, J., Brouwer, P.A., Emmer, B.J., de Bruijn, S.F., van Dijk, L.C., Kappelle, L.J., Lo, R.H., van Dijk, E.J., de Vries, J., de Kort, P.L.M., van Rooij, W.J.J., van den Berg, J.S.P., van Hasselt, B.A.A.M., Aerden, L.A.M., Dallinga, R.J., Visser, M.C., Bot, J.C.J., Vroomen, P.C., Eshghi, O., Schreuder, T.H.C.M.L., Heijboer, R.J.J., Keizer, K., Tielbeek, A.V., den Hertog, H.M., Gerrits, D.G., van den Berg-Vos, R.M., Karas, G.B., Steyerberg, E.W., Flach, H.Z., Marquering, H.A., Sprengers, M.E.S., Jenniskens, S.F.M., Beenen, L.F.M., van den Berg, R., Koudstaal, P.J., van Zwam, W.H., Roos, Y.B.W.E.M., van der Lugt, A., van Oostenbrugge, R.J., Majoie, C.B.L.M., Dippel, D.W.J., 2015. A randomized trial of intraarterial treatment for acute ischemic stroke. *N. Engl. J. Med.* 372 (1), 11–20.
- Berndt, M., Friedrich, B., Maegerlein, C., Moench, S., Hedderich, D., Lehm, M., Zimmer, C., Straeter, A., Poppert, H., Wunderlich, S., Schirmer, L., Oberdieck, P., Kaesmacher, J., Boeckh-Behrens, T., 2018. Thrombus permeability in admission computed tomographic imaging indicates stroke pathogenesis based on thrombus histology. *Stroke* 49 (11), 2674–2682.
- Booth, N.A., Simpson, A.J., Croll, A., Bennett, B., MacGregor, I.R., 1988. Plasminogen activator inhibitor (PAI-1) in plasma and platelets. *Br. J. Haematol.* 70 (3), 327–333.
- Choi, M.H., Park, G.H., Lee, J.S., Lee, S.E., Lee, S.-J., Kim, J.-H., Hong, J.M., 2018. Erythrocyte fraction within retrieved thrombi contributes to thrombolytic response in acute ischemic stroke. *Stroke* 49 (3), 652–659.
- Clague, D.S., Kandhai, B.D., Zhang, R., Slood, P.M.A., 2000. Hydraulic permeability of (un)bounded fibrous media using the lattice Boltzmann method. *Phys. Rev. E* 61 (1), 616–625.
- Davies, C.N., 1952. The separation of airborne dust and particles. *Inst. Mech. Eng.* B1, 185–213.
- Diamond, S.L., 1999. Engineering design of optimal strategies for blood clot dissolution. *Annu. Rev. Biomed. Eng.* 1 (1), 427–461.
- Diamond, S.L., Anand, S., 1993. Inner clot diffusion and permeation during fibrinolysis. *Biophys. J.* 65 (6), 2622–2643.
- Dutra, B.G., Tolhuisen, M.L., Alves, H.C.B.R., Treurniet, K.M., Kappelhof, M., Yoo, A.J., Jansen, I.G.H., Dippel, D.W.J., van Zwam, W.H., van Oostenbrugge, R.J., da Rocha, A.J., Lingsma, H.F., van der Lugt, A., Roos, Y.B.W.E.M., Marquering, H.A., Majoie, C.B.L.M., the MR CLEAN Registry Investigators, 2019. Thrombus imaging characteristics and outcomes in acute ischemic stroke patients undergoing endovascular treatment. *Stroke* 50 (8), 2057–2064.
- Ethier, C.R., 1991. Flow through mixed fibrous porous materials. *AIChE J.* 37 (8), 1227–1236.
- Gu, B., Piebalgs, A., Huang, Y., Roi, D., Lobotesis, K., Longstaff, C., Hughes, A.D., Chen, R., Thom, S.A., Xu, X.Y., 2019. Computational simulations of thrombolysis in acute stroke: Effect of clot size and location on recanalisation. *Med. Eng. Phys.* 73, 9–17.
- Hoylaerts, M., Rijken, D.C., Lijnen, H.R., Collen, D., 1982. Kinetics of the activation of plasminogen by human tissue plasminogen activator. Role of fibrin. *J. Biol. Chem.* 257 (6), 2912–2919.
- INSIST consortium, 2017. In Silico clinical trials for treatment of acute ischemic stroke (INSIST) H2020 project. <https://insist-h2020.eu/>.
- Jackson, G.W., James, D.F., 1986. The permeability of fibrous porous media. *Can. J. Chem. Eng.* 64 (3), 364–374.
- Kim, Y.D., Nam, H.S., Kim, S.H., Kim, E.Y., Song, D., Kwon, I., Yang, S.-H., Lee, K., Yoo, J., Lee, H.S., Heo, J.H., 2015. Time-dependent thrombus resolution after tissue-type plasminogen activator in patients with stroke and mice. *Stroke* 46 (7), 1877–1882.
- Kim, P.Y., Stewart, R.J., Lipson, S.M., Nesheim, M.E., 2007. The relative kinetics of clotting and lysis provide a biochemical rationale for the correlation between elevated fibrinogen and cardiovascular disease. *J. Thromb. Haemost.* 5 (6), 1250–1256.
- Konduri, P.R., Marquering, H.A., van Bavel, E.E., Hoekstra, A., Majoie, C.B.L.M., The INSIST Investigators, 2020. In-silico trials for treatment of acute ischemic stroke. *Front. Neurol.* 11.
- Kotsalos, C., Latt, J., Chopard, B., 2019. Bridging the computational gap between mesoscopic and continuum modeling of red blood cells for fully resolved blood flow. *J. Comput. Phys.* 398, 108905.
- Krüger, T., Kusumaatmaja, H., Kuzmin, A., Shardt, O., Silva, G., Viggien, E.M., 2017. The Lattice Boltzmann method: Principles and practice. In: Graduate Texts in Physics. Springer International Publishing, Cham.
- Lansberg, M.G., Bluhmki, E., Thijs, V.N., 2009. Efficacy and safety of tissue plasminogen activator 3 to 4.5 hours after acute ischemic stroke: A metaanalysis. *Stroke* 40 (7), 2438–2441.
- Latt, J., Malaspinas, O., Kontaxakis, D., Parmigiani, A., Lagrava, D., Brogi, F., Belgacem, M.B., Thorimbert, Y., Leclaire, S., Li, S., Marson, F., Lemus, J., Kotsalos, C., Conradin, R.A., Coreixas, C., Petkantchin, R., Raynaud, F., Beny, J.A., Chopard, B., 2020. Palabos: Parallel lattice Boltzmann solver. *Comput. Math. Appl.*
- Li, S., Chopard, B., Latt, J., 2019. Continuum model for flow diverting stents in 3D patient-specific simulation of intracranial aneurysms. *J. Comput. Sci.* 38, 101045.
- Malaspinas, O., Turjman, A., Ribeiro de Sousa, D., Garcia-Cardena, G., Raes, M., Nguyen, P.-T.T., Zhang, Y., Courbebaisse, G., Lelubre, C., Zouaoui Boudjeltia, K., Chopard, B., 2015. A spatio-temporal model for spontaneous thrombus formation in cerebral aneurysms. *bioRxiv*.
- Miyazaki, H., Yamaguchi, T., 2003. Formation and destruction of primary thrombi under the influence of blood flow and Von Willebrand factor analyzed by a discrete element method. *Biorheology* 40 (1,2,3), 265–272.
- Mosnier, L.O., Buijtenhuijs, P., Marx, P.F., Meijers, J.C.M., Bouma, B.N., 2003. Identification of thrombin activatable fibrinolysis inhibitor (TAFI) in human platelets. *Blood* 101 (12), 4844–4846.
- Padmos, R.M., Józsa, T.I., El-Bouri, W.K., Konduri, P.R., Payne, S.J., Hoekstra, A.G., 2021. Coupling one-dimensional arterial blood flow to three-dimensional tissue perfusion models for in silico trials of acute ischaemic stroke. *Interface Focus* 11 (1), 20190125.
- Piebalgs, A., Gu, B., Roi, D., Lobotesis, K., Thom, S., Xu, X.Y., 2018. Computational simulations of thrombolytic therapy in acute ischaemic stroke. *Sci. Rep.* 8 (1).
- Piebalgs, A., Xu, X.Y., 2015. Towards a multi-physics modelling framework for thrombolysis under the influence of blood flow. *J. R. Soc. Interface* 12 (113), 20150949.
- Prasad, S., Kashyap, R.S., Deopujari, J.Y., Purohit, H.J., Taori, G.M., Dagainawala, H.F., 2006. Development of an in vitro model to study clot lysis activity of thrombolytic drugs. *Thromb. J.* 4 (1), 14.
- Qazi, E.M., Sohn, S.I., Mishra, S., Almekhlafi, M.A., Eesa, M., d'Esterre, C.D., Qazi, A.A., Puig, J., Goyal, M., Demchuk, A.M., Menon, B.K., 2015. Thrombus characteristics are related to collaterals and angioarchitecture in acute stroke. *Can. J. Neurol. Sci. (J. Can. des Sci. Neurol.)* 42 (6), 381–388.
- Raynaud, F., Rousseau, A., Daniel, M., Perez-Morga, D., Zouaoui Boudjeltia, K., Chopard, B., Chopard, B., 2021. Investigating the two regimes of fibrin clot lysis: An experimental and computational approach. *Biophys. J.*
- Reed, M., Kerndt, C.C., Nicolas, D., 2020. Alteplase. In: StatPearls. StatPearls Publishing, Treasure Island (FL).
- Rijken, D.C., Hoylaerts, M., Collen, D., Fibrinolytic properties of one-chain and two-chain human extrinsic (tissue-type) plasminogen activator. 6.
- Rull, G., Thrombolytic treatment of acute ischaemic stroke, Patient.
- Santos, E.M.M., Dankbaar, J.W., Treurniet, K.M., Horsch, A.D., Roos, Y.B., Kappelle, L.J., Niessen, W.J., Majoie, C.B., Velthuis, B., Marquering, H.A., Duijlm, L.E., Keizer, K., van der Lugt, A., Dippel, D.W., Droogh de Greeve, K.E., Bienfait, H.P., van Walderveen, M.A., Wermer, M.J., Lycklama à Nijeholt, G.J., Boiten, J., Duyndam, D., Kwa, I.V., Meijer, J.F., van Dijk, E.J., Kesselring, F.O., Hofmeijer, J., Vos, J.A., Schonewille, W.J., van Rooij, W.J., de Kort, P.L., Pleiter, C.C., Bakker, S.L., Bot, J., Visser, M.C., van der Schaaf, I.C., Mali, W.P., van Seeters, T., Niesten, J.M., Biessels, G.J., Luitse, M.J., van der Graaf, Y., 2016a. Permeable thrombi are associated with higher intravenous recombinant tissue-type plasminogen activator treatment success in patients with acute ischemic stroke. *Stroke* 47 (8), 2058–2065.
- Santos, E.M.M., Marquering, H.A., den Blanken, M.D., Berkhemer, O.A., Boers, A.M.M., Yoo, A.J., Beenen, L.F., Treurniet, K.M., Wismans, C., van Noort, K., Lingsma, H.F., Dippel, D.W.J., van der Lugt, A., van Zwam, W.H., Roos, Y.B.W.E.M., van Oostenbrugge, R.J., Niessen, W.J., Majoie, C.B., on behalf of the MR CLEAN Investigators, Fransen, P.S.S., Beumer, D., van den Berg, L.A., Schonewille, W.J., Vos, J.A., Nederkoorn, P.J., Wermer, M.J.H., van Walderveen, M.A.A., Staals, J., Hofmeijer, J., van Oostayen, J.A., Lycklama à Nijeholt, G.J., Boiten, J., Brouwer, P.A., Emmer, B.J., de Bruijn, S.F., van Dijk, L.C., Kappelle, L.J., Lo, R.H., van Dijk, E.J., de Vries, J., de Kort, P.L.M., van den Berg, J.S.P., van Hasselt, B.A.A.M., Aerden, L.A.M., Dallinga, R.J., Visser, M.C., Bot, J.C.J., Vroomen, P.C., Eshghi, O., Schreuder, T.H.C.M.L., Heijboer, R.J.J., Keizer, K., Tielbeek, A.V., den Hertog, H.M., Gerrits, D.G., van den Berg-Vos, R.M., Karas, G.B., Sprengers, M.E.S., Jenniskens, S.F.M., van den Berg, R., Koudstaal, P.J., Boiten, J., van Dijk, E.J., Wermer, M.J.H., Flach, H.Z., Steyerberg, E.W., Brown, M.M., Liebig, T., Stijnen, T., Andersson, T., Mattle, H.P., Wahlgren, N., Koudstaal, P.J., van der Heijden, E., Ghannouti, N., Fleitour, N., Hooijenga, I., Lindl-Vealema, A., Puppels, C., Pelikaan, W., Jansen, K., Aaldering, N., Elfrink, M., de Meris, J., Geerlings, A., van Vemde, G., de Ridder, A., Greebe, P., de Bont-Stikkelbroeck, J., Struijk, W., Simons, T., Messchendorp, G., van der Minne, F., Bongenaar, H., Bodde, K., Licher, S., Boodt, N., Ros, A., Venema, E., Slokkers, I., Ganpat, R.-J., Mulder, M., Saiedie, N., Heshmatollah, A., Schipperen, S., Vinken, S., van Boxtel, T., Koets, J., Boers, M., Borst, J., Jansen, I., Kappelhof, M., Lucas, M., Geuskens, R., Barros, R.S., Dobbe, R., Cszimadia, M., 2016b. Thrombus permeability is associated with

- improved functional outcome and recanalization in patients with ischemic stroke. *Stroke* 47 (3), 732–741.
- Shibeko, A.M., Chopard, B., Hoekstra, A.G., Pantelev, M.A., 2020. Redistribution of TPA fluxes in the presence of PAI-1 regulates spatial thrombolysis. *Biophys. J.* 119 (3), 638–651.
- Sorimachi, T., Fujii, Y., Tsuchiya, N., Nashimoto, T., Saito, M., Morita, K., Ito, Y., Tanaka, R., 2005. Blood pressure in the artery distal to an intraarterial embolus during thrombolytic therapy for occlusion of a major artery: A predictor of cerebral infarction following good recanalization. *J. Neurosurg.* 102 (5), 870–878.
- Sorimachi, T., Morita, K., Ito, Y., Fujii, Y., 2011. Blood pressure measurement in the artery proximal and distal to an intra-arterial embolus during thrombolytic therapy. *J. Neuro Interv. Surg.* 3 (1), 43–46.
- Staessens, S., De Meyer, S.F., 2020. Thrombus heterogeneity in ischemic stroke. *Platelets* 1–9.
- Staessens, S., Denorme, F., Francois, O., Desender, L., Dewaele, T., Vanacker, P., Deckmyn, H., Vanhoorelbeke, K., Andersson, T., De Meyer, S.F., 2020. Structural analysis of ischemic stroke thrombi: Histological indications for therapy resistance. *Haematologica* 105 (2), 498–507.
- Tutwiler, V., Mukhitov, A.R., Peshkova, A.D., Le Minh, G., Khismatullin, R.R., Vicksman, J., Nagaswami, C., Litvinov, R.I., Weisel, J.W., 2018. Shape changes of erythrocytes during blood clot contraction and the structure of polyhedrocytes. *Sci. Rep.* 8 (1), 17907.
- Walsh, S.D.C., Burwinkle, H., Saar, M.O., 2009. A new partial-bounceback Lattice-Boltzmann method for fluid flow through heterogeneous media. *Comput. Geosci.* 35 (6), 1186–1193.
- Whyte, C.S., Swieringa, F., Mastenbroek, T.G., Lionikiene, A.S., Lancé, M.D., van der Meijden, P.E.J., Heemskerck, J.W.M., Mutch, N.J., 2015. Plasminogen associates with phosphatidylserine-exposing platelets and contributes to thrombus lysis under flow. *Blood* 125 (16), 2568–2578.
- Wu, J.H., Siddiqui, K., Diamond, S.L., 1994. Transport phenomena and clot dissolving therapy: An experimental investigation of diffusion-controlled and permeation-enhanced fibrinolysis. *Thromb. Haemost.* 72 (1), 105–112.
- Wufsus, A.R., Macera, N.E., Neeves, K.B., 2013. The hydraulic permeability of blood clots as a function of fibrin and platelet density. *Biophys. J.* 104 (8), 1812–1823.
- Wufuer, A., Wubuli, A., Mijiti, P., Zhou, J., Tuerxun, S., Cai, J., Ma, J., Zhang, X., 2017. Impact of collateral circulation status on favorable outcomes in thrombolysis treatment: A systematic review and meta-analysis. *Exp. Ther. Med.*
- Zhou, Y., Murugappan, S.K., Sharma, V.K., 2014. Effect of clot aging and cholesterol content on ultrasound-assisted thrombolysis. *Transl. Stroke Res.* 5 (5), 627–634.